Proceedings of the 8th IEEE Mediterranean Conference
on Control and Automation (MED 2000)
Rio, Patras, GREECE 17-19 July, 2000

LOCAL AND GLOBAL BIFURCATIONS IN A POWER SYSTEM WITH TWO CASCADED REGULATORS

G. A. MANOS **D. MAKRIDOU** **C. D. VOURNAS**

Electrical Energy Systems Lab., Dept. of Electrical & Computer Eng.
National Technical University
P.O.Box 26137, Athens GR-100 22, Greece
e - mail vournas@power.ece.ntua.gr

Abstract. This paper investigates local and global bifurcation phenomena in a power system with two cascaded Load Tap Changer transformers. These devices regulate voltage at two different voltage levels. Conditions for oscillatory behavior and the stability of the system are extracted. The interaction between the two devices is also considered. More specifically, it is shown how the cascaded time constants influence the monotonic or oscillatory behavior of the system and the formation of a homoclinic loop bifurcation.

Key Words. Power system control, cascaded regulators, bifurcations, limit cycle, homoclinic loop.

1. INTRODUCTION

Power systems are highly nonlinear dynamical systems. The nonlinear models describing power systems can exhibit a wide variety of complex behavior [1-3]. Moreover economic and environmental restrictions, along with the current trend to open the power market, force modern power systems to operate ever closest to their stability limits. Consequently, power systems behavior becomes even more dependent on nonlinear characteristics and more complex. A great effort has been spent recently in analyzing these nonlinear phenomena [4-6].

Load restoration dynamics play a significant role in voltage instability phenomena [3,5,7,13]. An important mechanism of load restoration is that of Load Tap Changers (LTCs). These devices regulate load voltages and therefore they restore indirectly load power, even when transmission system voltages are reduced. Voltage instability problems initiated by LTC dynamics are analyzed in [7,8,10], using both discrete and/or continuous LTC models. Oscillatory behavior produced by the interaction between cascaded tap changing transformers has been noticed in [1,9,13]. It has been mentioned that these oscillations appear when the time constants of all LTCs belong to the same time frame. In [12], the appearance of a limit cycle has been observed as a result of the interaction between load and LTC dynamics.

In this paper we analyze extensively from a stability point of view a system with two cascaded LTCs in both parameter and state space. The analysis is performed using bifurcation theory. More specifically, we derive conditions for:

- Oscillatory behavior
- Hopf Bifurcation
- Saddle Node Bifurcation

Apart from these local bifurcations we investigate also a global bifurcation, namely a Homoclinic Loop Bifurcation (HLB).

Although LTC dynamics are discrete, we use equivalent continuous models in order to perform stability analysis. In [3,8] methods to provide straight forward derivations of continuous tap dynamic models from basic discrete ones are presented. These methods consist of the identification of the appropriate form and time constant data for continuous - tap dynamic models.

2. BIFURCATIONS

The term *bifurcation* refers to the points in parameter space, for which the qualitative structure of the system changes for a small variation of a parameter vector. More specifically:

- At *Local Bifurcations* the change of the qualitative structure of the system refers to local properties, such as stability of equilibria and periodic orbits.
- At *Global Bifurcations* the qualitative structure of the system changes globally in the state space,

i.e. it is not restricted in the neighborhood of an equilibrium point.

A *Saddle Node Bifurcation* occurs when a stable - unstable pair of equilibrium points disappears or emerges simultaneously. In power systems, this bifurcation usually coincides with a maximum power transfer point of the system. At this bifurcation, the state matrix of the system becomes singular.

A *Hopf bifurcation* causes the emergence or disappearance of a periodic solution through its interaction with an equilibrium point. At this bifurcation, a pair of complex conjugate eigenvalues of the state matrix crosses the imaginary axis. There are two distinct types of Hopf bifurcation depending on the stability of the limit cycle:

- At a *subcritical* Hopf bifurcation an unstable limit cycle collides with a stable equilibrium. After the bifurcation the equilibrium becomes unstable and the limit cycle disappears.
- At a *supercritical* Hopf bifurcation a stable equilibrium point becomes unstable and a stable limit cycle is generated.

At a *Homoclinic Loop Bifurcation* one branch of the stable manifold and one branch of the unstable manifold of the same unstable equilibrium point coincide. An isolated closed trajectory (loop), passing through the unstable equilibrium point, is generated. This trajectory is called a homoclinic loop. After this bifurcation an unstable limit cycle is generated.

3. THE TWO CASCADED LTCs SYSTEM

3.1. System description

The system studied in this paper consists of a constant voltage source (infinite bus) feeding an isolated load (purely resistive), through a lossless transmission line and two transformers equipped with LTCs. The reactances of the two transformers are X_1 and X_2 respectively. The system is shown in the one line diagram of Fig. 1. The transmission line connects the infinite bus to the transformer through a total reactance X_o. The reactive losses of the two transformers (i.e. on reactances X_1 and X_2) are compensated by a capacitor (of admittance B). Table 1 shows the network and system parameters (pu on 100MVA base).

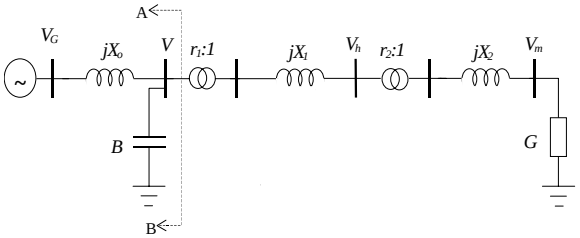

Figure 1: The two cascaded LTCs power system

Table 1: Network, Load and LTCs parameters

X_o	X_1	X_2	B	V_G	V_h^o	V_m^o
0.1	0.2	0.15	3.33	1.036	1.0	1.0

The load is represented as a constant admittance G. The LTC dynamics are described by the following two differential equations (continuous model):

$$\dot{r}_1 = \frac{1}{T_1}(V_h - V_h^0) \quad (1)$$

$$\dot{r}_2 = \frac{1}{T_2}(V_m - V_m^0) \quad (2)$$

where:

r_1, r_2 are the tap positions (state variables)

V_h^0, V_m^0 are the secondary voltage set points

T_1, T_2 are the corresponding time constants

As seen in (1), (2) the LTC controllers are integral regulators.

The secondary voltages V_h and V_m of the transformers are given by the following expressions:

$$V_h^2 = g(r_1, r_2)E_T^2 \quad (3)$$

$$V_m^2 = h(r_1, r_2)E_T^2 \quad (4)$$

where:

$$g(r_1, r_2) = \frac{r_1^2 r_2^4 + G^2 r_1^2 r_2^4 X_2^2}{r_1^4 r_2^4 + G^2\left(X_T + r_1^2 X_1 + r_1^2 r_2^2 X_2\right)^2}$$

$$h(r_1, r_2) = \frac{r_1^2 r_2^2}{r_1^4 r_2^4 + G^2\left(X_T + r_1^2 X_1 + r_1^2 r_2^2 X_2\right)^2}$$

where E_T, X_T are the Thevenin equivalent voltage and reactance at A, B (see Fig. 1). Note, that the time constants T_1, T_2 and the load admittance G are considered as the variable parameters of our system.

3.2. Equilibrium Conditions

The equilibrium points of the system are defined by the following nonlinear algebraic equations:

$$V_h(r_1, r_2) - V_h^0 = 0 \quad (5)$$

$$V_m(r_1, r_2) - V_m^0 = 0 \quad (6)$$

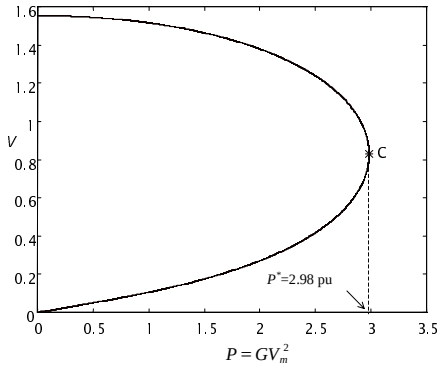

Figure 2: PV curve of the system

where V_h, V_m are given by (3), (4). From the solution of the above system we can find two pairs of equilibria, one corresponding to normal transmission system voltage and one corresponding to low voltage.

In Fig. 2, we can see the equilibrium points of the system for various loading levels, in terms of a *PV* curve. In the same figure, P $(= GV_m^2)$ is the power

consumed by the load and V is the transmission voltage close to the infinite bus (see Fig. 1).
The following remarks can be made on Fig. 2:

- For $P < P^*(=2.98\,pu)$ the system has two equilibrium points, one corresponding to high voltage V and one corresponding to a low value of voltage V.
- For $P = P^*$ the two equilibrium points coalesce and disappear. This point is a Saddle Node Bifurcation of the system.
- For $P > P^*$ the system has no equilibrium points.

3.3. Linearization

Linearizing around an equilibrium point, the system (1) – (2) becomes:

$$\begin{bmatrix} \Delta\dot{r}_1 \\ \Delta\dot{r}_2 \end{bmatrix} = \mathbf{T}^{-1}\mathbf{A}\begin{bmatrix} \Delta r_1 \\ \Delta r_2 \end{bmatrix} \tag{7}$$

where:

$$\mathbf{A} = \begin{bmatrix} A_{11} & A_{12} \\ A_{21} & A_{22} \end{bmatrix}$$

$$\mathbf{T} = \begin{bmatrix} T_1 & 0 \\ 0 & T_2 \end{bmatrix}$$

and

$$A_{11} = \frac{V_G^{\,2}}{2V_h^0}\frac{\partial g}{\partial r_1}, \quad A_{12} = \frac{V_G^{\,2}}{2V_h^0}\frac{\partial g}{\partial r_2}$$

$$A_{21} = \frac{V_G^{\,2}}{2V_m^0}\frac{\partial h}{\partial r_1}, \quad A_{22} = \frac{V_G^{\,2}}{2V_m^0}\frac{\partial h}{\partial r_2}$$

Note that, A_{11}, A_{12}, A_{21}, A_{22} are functions of load admittance G. At this point we remark that $A_{11} < 0$ for all values of G, whereas A_{22} changes sign depending on G.
The matrix:

$$\mathbf{A}' = \mathbf{T}^{-1}\mathbf{A} \tag{8}$$

is the state matrix of the system.
The characteristic polynomial of the system is given by [9]:

$$\lambda^2 - \left(\frac{A_{22}}{T_2} + \frac{A_{11}}{T_1}\right)\lambda + \left(\frac{D_A}{T_1T_2}\right) = 0 \tag{9}$$

where:

$$D_A = A_{11}A_{22} - A_{12}A_{21} \tag{10}$$

is the determinant of **A**.

4. LOCAL CONDITIONS FOR OSCILLATORY BEHAVIOR AND STABILITY

4.1. Oscillation Condition

We want here to derive the region in parameter space, where the system exhibits oscillatory behavior.

According to the characteristic polynomial (9), the damping factor ζ of the system is given by:

$$\zeta = \frac{-\left(A_{22}\gamma + \dfrac{A_{11}}{\gamma}\right)}{2\sqrt{D_A}} \tag{11}$$

where: $\gamma = \sqrt{T_1/T_2}$

For a given load admittance G and provided that $A_{11}A_{22} > 0$, it is easily shown that the damping factor • has a local minimum with respect to γ, given by:

$$\zeta_{\min} = \sqrt{\frac{A_{11}A_{22}}{D_A}} \tag{12}$$

Considering that A_{11} is always negative (for all values of G), (12) holds as long as $A_{22} < 0$.

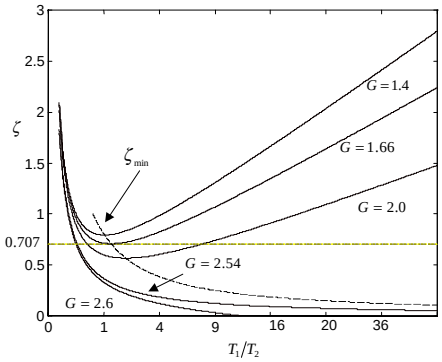

Figure 3: Variation of damping factor

In Fig. 3 we can see the variation of damping factor • as a function of the ratio T_1/T_2, for different values of the load admittance G. In the same figure, the dotted line shows the minimum value $\zeta_{\min}$ for a given G.

Note that, for $G \geq 2.54$, A_{22} becomes positive ($A_{22} \geq 0$), so $\zeta_{\min}$ can not be defined.

We consider that, near the equilibrium the system exhibits monotonic behavior regardless of time constants T_1, T_2 as long as the following conditions hold:

- The damping factor • has a local minimum $\zeta_{\min}$ with respect to γ.
- The local minimum value $\zeta_{\min}$ is greater than 0.707.

The threshold value of $\zeta_{\min} = 0.707$ is chosen because it corresponds to a second-order linear system that does not exhibit overshoot. These conditions refer to local oscillations (close to the stable equilibrium point).

As shown in Fig. 3, for loading level bellow $G = 1.66\,pu$ there are no local oscillations. For higher values of the load, local oscillatory behavior depends on the relative speed of the two regulating mechanisms, i.e. on the ratio of time constants T_1/T_2.

In Fig. 4, the boundary of local oscillations is shown as curve 1 in the parameter space of G and T_1/T_2.

4.2. Stability Conditions

The stability conditions of system (7) are:

I. $tr\mathbf{A}' < 0$

II. $\det \mathbf{A}' > 0$

According to (8) the trace of the state matrix $\mathbf{A}'$ is given by:

$$tr\mathbf{A}' = \frac{A_{22}}{T_2} + \frac{A_{11}}{T_1} \tag{13}$$

Note that:

- As long as $A_{22} < 0$ (given that $A_{11} < 0$) stability condition (I) holds regardless of the values of time constants T_1 and T_2.
- If $A_{22} \geq 0$ (this holds for load admittance $G \geq 2.54$), there are time constants values T_1, T_2 for which condition (I) is violated.

According to (13) and condition (I), the stability in terms of T_1/T_2 (for $G \geq 2.54$) is defined by:

$$\frac{T_1}{T_2} < \frac{|A_{11}|}{A_{22}} \tag{14}$$

And the stability boundary is given by:

$$\frac{T_1}{T_2} = \frac{|A_{11}|}{A_{22}} \tag{15}$$

Relation (15) is the condition for Hopf bifurcation (where a pair of conjugate eigenvalues of $\mathbf{A}'$ crosses the imaginary axis). After the Hopf bifurcation the system becomes *oscillatory unstable*.

When stability condition (II) is violated, the system encounters a Saddle Node Bifurcation, and the state matrix $\mathbf{A}'$ becomes singular.

Note that, matrices $\mathbf{A}'$ and $\mathbf{A}'$ become singular simultaneously ($\det \mathbf{A}' = \det \mathbf{A}$), therefore the condition for Saddle Node Bifurcation is:

$$\det \mathbf{A} = 0 \tag{16}$$

5. ANALYSIS IN THE PARAMETER SPACE

From the preceding analysis we can plot the stability and oscillatory regions in the parameter space of load admittance G and time constant ratio T_1/T_2 (as in Fig. 4). From Fig. 4 we conclude the following:

- For light loading conditions $(G < 1.66)$:
  - The system does not exhibit oscillatory behavior near the equilibrium point (for any combination of time constants T_1, T_2).
  - The equilibrium point is stable.
- For medium loading conditions $(1.66 < G \leq 2.54)$:
  - There is a local oscillatory region in the parameter space (to the right and above curve 1 in Fig. 4).
  - The equilibrium is stable (for any combination of time constants T_1, T_2).
- High loading conditions $(G > 2.54)$
  - The stable monotonic region in the parameter space shrinks.
  - There is a region in the parameter space where the equilibrium is unstable. This happens after a Hopf bifurcation (curve 2 in Fig. 4) is encountered.

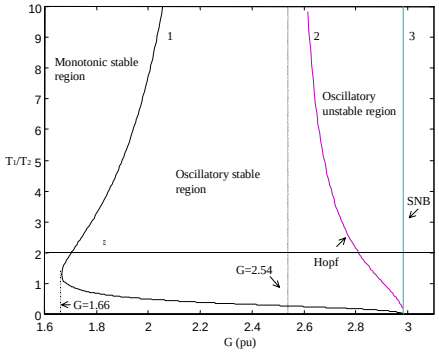

Figure 4: Oscillatory and stability region in parameter space

- For loading above the Saddle Node Bifurcation value $G = 2.98\,pu$ there is no longer an equilibrium.

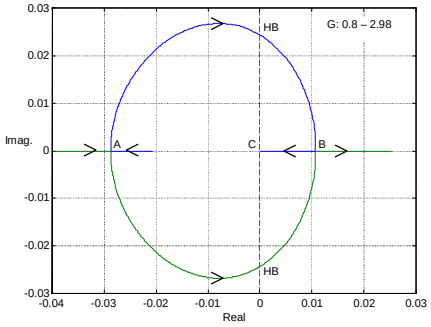

Figure 5: Eigenvalues of the system (T_1=40s, T_2=20s)

The eigenvalues of the linearized system (7), for specific values of time constants (T_1 *=40sec*, T_2 *=20sec*) and increasing load admittance *G*, are plotted in Fig. 5, in the form of a root locus. For this plot the parameters move along line • in parameter space (see Fig. 4).

From Fig. 5 we notice the following:

- At point A (*G=0.96pu*) the two real eigenvalues of the system become complex.
- At point HB (*G=2.81pu*) the imaginary axis is crossed. This is a Hopf bifurcation of the system.
- At point B (*G=2.97pu*) the complex eigenvalues become real again.
- After point B one real eigenvalue becomes zero at point C (*G=2.98pu*). This is the Saddle Node Bifurcation of the system. There are no equilibrium points after this value of *G*.

6. ANALYSIS IN THE STATE SPACE

In previous sections the local behavior of the system near its stable equilibrium point was investigated. In this section, we perform simulations to investigate

global dynamics of the system, e.g. the region of attraction of the stable equilibrium point, limit cycles, global bifurcations etc.

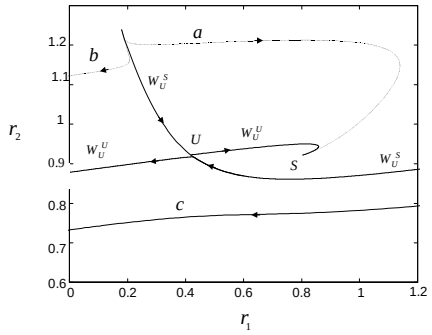

Figure 6: Monotonic behavior (T_1/T_2 =0.1)

The simulations are performed for a load admittance G=2.8pu. For this loading the system has two equilibrium points. One corresponding to high network voltages ($\bar{r}_1 = 0.8036$, $\bar{r}_2 = 0.9220$) and one corresponding to low network voltages ($\bar{r}_1 = 0.4180$, $\bar{r}_2 = 0.9220$). Note that, equilibrium points are independent on the time constants T_1 , T_2 .

In Fig. 6, the phase portrait of the system, for T_1 =5sec, T_2 =50sec (T_1/T_2 =0.1), is depicted. In this case, where the first LTC is fast enough compared to the second, the system exhibits monotonic response near the stable equilibrium point *S*.

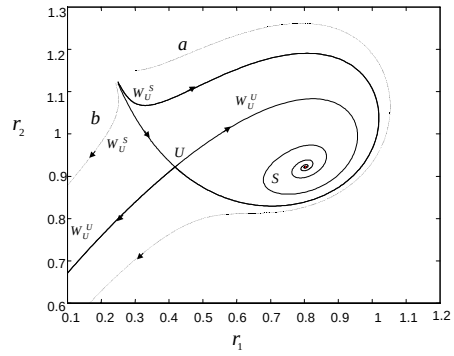

Figure 7: Phase portrait before the Homoclinic Loop Bifurcation (T_1/T_2 =1.0)

Point *U* is the unstable equilibrium point (saddle point). The region of attraction of point *S* is bounded by the two branches of the stable manifold (W_U^S) of the unstable equilibrium *U* (see Fig. 6).

By increasing time constant T_1 (T_1 =50sec) we have the phase portrait of Fig. 7. In this case the dynamics of both LTCs belong to the same time scale. The system exhibits oscillatory behavior in the region of attraction of the asymptotically stable equilibrium point *S*. This region is bounded by the stable manifold (W_U^S) of the unstable equilibrium *U* (see Fig. 7). Outside this region, the response of the system is unstable (see trajectories *a* and *b* in Fig. 7).

For further increase of time constant T_1 (T_1 =64.4sec) we have the phase portrait of Fig. 8. From this phase portrait we can see that one branch of the stable manifold (W_U^S) and one branch of the unstable manifold (W_U^U) of the unstable equilibrium point coincide, i.e. an isolated closed trajectory, passing through the unstable equilibrium point, is generated (*homoclinic loop*). At this point the system is structurally unstable (in the sense that any small parameter variation will break the homoclinic loop) and undergoes a *Homoclinic Loop Bifurcation.* After this bifurcation an unstable limit cycle, surrounding the stable equilibrium point is generated.

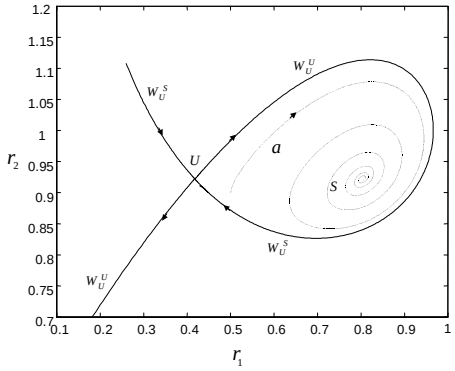

Figure 8: Homoclinic Loop Bifurcation (T_1/T_2 =1.29)

The homoclinic loop bounds the region of attraction of the stable equilibrium point, where the response of the system is oscillatory (see trajectory a in Fig. 8). Outside this region, the response of the system is monotonically unstable.

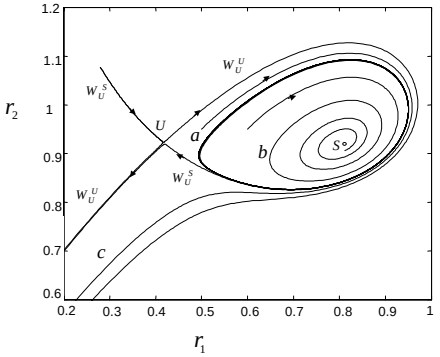

Figure 9: Emergence of unstable limit cycle after the Homoclinic Loop Bifurcation (T_1/T_2 =1.42)

For further increase of time constant T_1 (T_1 =71sec) we have the phase portrait of Fig. 9. In this phase portrait we can see the emergence of the unstable limit cycle (after the breaking of the homoclinic loop). Now, this limit cycle bounds the region of attraction of the stable equilibrium point. Outside this region system trajectories are unstable.

In Fig. 10 we can see the phase portrait of the system prior to the Hopf Bifurcation (note that at this bifurcation the unstable limit cycle coalesces with the stable equilibrium point). This phase portrait is extracted for time constant T_1 =90sec. Outside the limit cycle the response of the system is initially oscillatory and becomes monotonically after the stable manifold W_U^S (of the unstable equilibrium point *U*) is overtaken (see Fig. 10). The Hopf

Bifurcation is *subcritical* since the limit cycle prior to the bifurcation is unstable and shrinks.

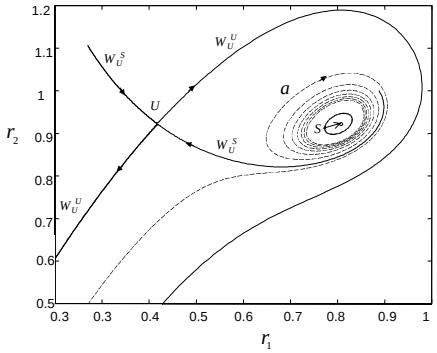

Figure 10: Shrinking Limit Cycle prior to Hopf Bifurcation (T_1/T_2 =1.8)

7. CONCLUSIONS

In this paper local and global bifurcations in a power system with two cascaded Load Tap Changer transformers were investigated. The analysis was performed in both parameter and state space. Conditions for oscillatory behavior and the stability of the equilibrium point were extracted.

The system encounters three types of bifurcations for changing loading and time constants:

- Two local bifurcations (Hopf Bifurcation and Saddle Node Bifurcation).
- One global bifurcation (Homoclinic Loop Bifurcation).

Before the Saddle Node Bifurcation, the system has two equilibrium points, one corresponding to high network voltage and one corresponding to low network voltage (which is always unstable). The former equilibrium point is stable until a Hopf Bifurcation is met. More specifically, for loading above $G = 2.54$, the system will exhibit oscillations near the stable equilibrium point if the time constants of the two LTCs are close enough. Also for a certain value of the ratio T_1/T_2 the system will undergo a Hopf Bifurcation becoming unstable. Note that, this bifurcation is the actual stability limit of the system since the Saddle Node Bifurcation occurs always after the Hopf Bifurcation.

Regarding the global dynamics of the system we note the following:

- Prior to the Homoclinic Loop Bifurcation, the region of attraction of the stable equilibrium point is bounded by the stable manifold of the unstable equilibrium point.
- After the Homoclinic Loop Bifurcation and prior to Hopf Bifurcation the region of attraction of the stable equilibrium point is bounded by the unstable limit cycle, which surrounds it.
- After the Hopf Bifurcation there is no stable equilibrium point any longer.

8. REFERENCES

1. C. W. Taylor, *"Power System Voltage Stability"*, McGraw-Hill, 1994.
2. P. Kundur, *"Power System Stability and Control"*, McGraw-Hill, 1993.
3. T. Van Cutsem, C. D. Vournas, *"Voltage Stability of Electric Power Systems"*, Kluwer Academic Publishers, 1998.
4. H. G. Kwatny, R. F. Fischl, C. O. Nwankpa, "Local Bifurcation in Power Systems", Proceeding of the IEEE, November 1995, Vol. 83, No. 11, pp. 1456-1483.
5. M. A. Pai, P. W. Sauer, B. C. Lesieutre, R. Adapa *"Structural stability in power systems - effect of load models"*, IEEE Transactions on Power Systems, Vol. 10, pp. 609-615, May 1995.
6. V. Venkatasubramanian, H. Schattler, J. Zaborsky, *"Dynamics of Large Constrained Nonlinear Systems - A Taxonomy Theory"*, Proceedings of the IEEE, Vol. 83, No. 11, pp. 1530-1561, November 1995.
7. G. A. Manos, C. D. Vournas, "Voltage Stability of a synchronous generator feeding a restorative load", IEEE/KTH Stockholm Power Tech Conference '95, June 18-22 1995, Vol. 1, pp. 197-202.
8. P. W. Sauer, M. A. Pai, *"A Comparison of Discrete vs Continuous Dynamic Models of Tap - Changing - Under - Load Transformers"*, Proceedings: Bulk Power System Voltage Phenomena - III Seminar on Voltage Stability, Security & Control Davos pp. 643-650, 22-26 August 1994.
9. I. A. Hiskens, D. J. Hill, *"Dynamic interaction between tapping transformers"*, PSCC Proceedings, Vol. 2, Avignon, pp. 1027-1034, August 1993.
10. H. Ohtsuki, A. Yokoyama, Y. Sekine, *"Reverse Action of On-Load Tap Changer in Association with Voltage Collapse"*, IEEE Transactions on Power Systems, Vol. 6, No. 1, pp 300-306, February, 1991.
11. M.S. Calovic, *"Modeling and analysis of under-load tap-changing transformer control system"*, IEEE Transaction on Power Apparatus and Systems, Vol. 103, pp. 1909-1915, 1984.
12. Mats Larsson, *"Coordinated Tap Changer Control", Department of Industrial Electrical Engineering and Automation, Lund Institute of Technology, 1997.*
13. C. D. Vournas, T.Van Cutsem, *"Voltage oscillations with cascaded load restoration"*, Stocholm Power Tech Proceeding, Vol. Power Systems, p.p. 173-178, June 1995.